PROCEEDINGS OF SCIENCE

The effect of improved high-energy muon cross-sections

Jan Soedingrekso*, **Alexander Sandrock and Wolfgang Rhode**
Technische Universität Dortmund, Germany
E-mail: jan.soedingrekso@tu-dortmund.de,
alexander.sandrock@tu-dortmund.de

A precise simulation of muons with energies above a TeV is crucial for neutrino telescopes or cosmic ray experiments. To further increase the precision of these simulations, improved cross-section calculations are needed. At these energies, the interaction probability is dominated by bremsstrahlung for large energy losses and electron-positron pair production for small energy losses.
Improved analytical calculations for these processes were developed with more precise screening functions of the target atom as well as higher order corrections reducing the systematic uncertainties below the percent level. The new calculations are already implemented in the new version of the lepton propagator PROPOSAL, which was designed to be highly performant for the propagation through large volumes of media using interpolation tables and to do systematic studies with its multiple available cross-section calculations. The new calculations of the differential cross section result in a maximum deviation of 3 percent to the current standard. Their effects on the muon simulation with the resulting flux and energy loss distribution are presented.

36th International Cosmic Ray Conference -ICRC2019-
July 24th - August 1st, 2019
Madison, WI, U.S.A.

*Speaker.

© Copyright owned by the author(s) under the terms of the Creative Commons Attribution-NonCommercial-NoDerivatives 4.0 International License (CC BY-NC-ND 4.0).

PoS(ICRC2019)429

1. Improved cross sections

1.1 Leading-order bremsstrahlung cross section

The singly-differential cross section for bremsstrahlung of highly-relativistic leptons in the field of an atomic nucleus with charge Ze and mass Am_N can be expressed as [1]

$$d\sigma = 4\alpha \left(Z r_e \frac{m_e}{\mu} \right)^2 \frac{dv}{v} \left[(2 - 2v + v^2)\Phi_1(Z,A,\delta) - \frac{2}{3}(1-v)\Phi_2(Z,A,\delta) \right], \tag{1.1}$$

where μ refers to the mass of the lepton, m_e the electron mass, α is the fine structure constant and r_e the classical electron radius. v is the fractional energy loss of the lepton in the interaction. The dependence on the electric field of the nucleus is contained in the screening functions $\Phi_{1,2}$ which only depend on the nucleus and the minimum momentum transfer

$$\delta = \frac{\mu^2 v}{2E(1-v)}. \tag{1.2}$$

In the limiting case of complete screening and a point-like nucleus, the screening functions become independent of δ and are given by

$$\Phi_1^0 = \ln \left(B \frac{\mu}{m_e} Z^{-1/3} \right), \quad \Phi_2^0 = \Phi_1^0 - \frac{1}{6}. \tag{1.3}$$

Here, B is the radiation logarithm. In the Thomas-Fermi model, $B = 183$, while in the more exact Hartree-Fock model B depends on the nucleus. For the simulations, we use the Hartree-Fock radiation logarithms from [2]. In the absence of screening, the screening functions coincide for a point-like nucleus

$$\Phi_1^0 = \Phi_2^0 = \ln \frac{\mu}{\delta} - \frac{1}{2}. \tag{1.4}$$

In the approximation $\Phi_1 \approx \Phi_2$, an analytical interpolation was found by [3]

$$\Phi = \ln \frac{(\mu/m_e) B Z^{-1/3}}{1 + (\delta/m_e)\sqrt{e} B Z^{-1/3}} \tag{1.5}$$

which describes the intermediate behavior between complete screening and no screening for a point-like nucleus with high accuracy for medium and heavy nuclei.

The correction $\Delta_{1,2}$ for a nuclear form factor due to the finite size of the nucleus on the screening functions $\Phi^0_{1,2}$ is independent of screening, as very different regimes of transferred momenta to the nucleus are concerned, such that $\Phi_i = \Phi_i^0 - \Delta_i$.

Numerical results for the nuclear correction, calculated using a Fermi form factor with nuclear sizes according to [4], can be fitted with good accuracy using the expression

$$\Delta_1 = \ln \frac{\mu}{q_c} + \frac{\rho}{2} \ln \frac{\rho+1}{\rho-1}, \quad \Delta_2 = \ln \frac{\mu}{q_c} + \frac{3\rho - \rho^3}{4} \ln \frac{\rho+1}{\rho-1} + \frac{2\mu^2}{q_c^2} \tag{1.6}$$

with $\rho = \sqrt{1 + 4\mu^2/q_c^2}$, which follows from a step function for the nuclear form factor [5, 6]. Fitting to numerical results leads to $q_c = m_\mu e/D_n$ with $D_n = 1.54A^{0.27}$ (cf. [7]).

PoS(ICRC2019)429

We apply the interpolation analogous to [3] separately to $\Phi_{1,2}$ without assuming the screening functions to be equal. Adding the contributions due to the inelastic nuclear form factor [6] and the contribution from atomic electrons [8], we obtain the improved leading-order cross section for bremsstrahlung as

$$\begin{aligned}\frac{d\sigma}{dv} &= 4Z^2\alpha\left(r_e\frac{m_e}{\mu}\right)^2\frac{1}{v}\left\{\left[(2-2v+v^2)\Phi_1(\delta)-\frac{2}{3}(1-v)\Phi_2(\delta)\right]+\frac{1}{Z}s_{\text{atomic}}(v,\delta)\right\},\\ \Phi_1(\delta) &= \ln\frac{\frac{\mu}{m_e}BZ^{-1/3}}{1+BZ^{-1/3}\sqrt{e}\delta/m_e}-\Delta_1\left(1-\frac{1}{Z}\right),\\ \Phi_2(\delta) &= \ln\frac{\frac{\mu}{m_e}BZ^{-1/3}}{1+BZ^{-1/3}\sqrt[3]{e}\delta/m_e}-\Delta_2\left(1-\frac{1}{Z}\right),\\ s_{\text{atomic}}(v,\delta) &= \left[\frac{4}{3}(1-v)+v^2\right]\left[\ln\frac{\mu/\delta}{\mu\delta/m_e^2+\sqrt{e}}-\ln\left(1+\frac{m_e}{\delta B'Z^{-2/3}\sqrt{e}}\right)\right].\end{aligned} \tag{1.7}$$

1.2 Leading-order pair production cross section

The processes of pair production and bremsstrahlung are intimately connected. The discussion of the screening functions for bremsstrahlung can be analogously applied to the pair production process. However, an additional integration is carried out to obtain the doubly differential cross section $d^2\sigma/(dv\,d\rho)$ with $v=(E_++E_-)/E$, $\rho=(E_+-E_-)/(E_++E_-)$ designating the electron (positron) energy by $E_\pm$. The pair production cross section can be written as (cf. [9, 10])

$$\frac{d^2\sigma}{dv\,d\rho}=\frac{2}{3\pi}(Z\alpha r_e)^2\frac{1-v}{v}\left[C_eL_e+\frac{m_e^2}{\mu^2}C_\mu L_\mu\right] \tag{1.8}$$

with

$$C_e=[(2+\rho^2)(1+\beta)+\xi(3+\rho^2)]\ln\left(1+\frac{1}{\xi}\right)+\frac{1-\rho^2-\beta}{1+\xi}-(3+\rho^2), \tag{1.9}$$

$$C_\mu=\left[(1+\rho^2)\left(1+\frac{3}{2}\beta\right)-\frac{(1+2\beta)(1-\rho^2)}{\xi}\right]\ln(1+\xi)+\frac{\xi(1-\rho^2-\beta)}{1+\xi}+(1+2\beta)(1-\rho^2), \tag{1.10}$$

$$\beta=\frac{v^2}{2(1-v)},\quad \xi=\left(\frac{\mu v}{2m_e}\right)^2\frac{1-\rho^2}{1-v}. \tag{1.11}$$

The functions $L_{e,\mu}$ correspond to the screening functions integrated over the momentum transfer to the electron-positron-pair. This additional integration leads to terms not contained in the main logarithm which can be expressed in the limiting cases no screening and complete screening for a point-like nucleus by

$$\Phi_e^N=C_e\ln\frac{Ev(1-\rho^2)}{2m_e\sqrt{e}\sqrt{1+\xi}}-\frac{1}{2}|\Delta_e^N|, \tag{1.12}$$

$$\Phi_e^S=C_e\ln(BZ^{-1/3}\sqrt{1+\xi})+\frac{1}{2}\Delta_e^S, \tag{1.13}$$

PoS(ICRC2019)429

where [11]

$$|\Delta_e^N| = [(2+\rho^2)(1+\beta)+\xi(3+\rho^2)]\,\mathrm{Li}_2\frac{1}{1+\xi} - (2+\rho^2)\xi\ln\left(1+\frac{1}{\xi}\right) - \frac{\xi+\rho^2+\beta}{1+\xi}, \tag{1.14}$$

$$\Delta_e^S = |\Delta_e^N| - \frac{1}{6}\left\{[(1-\rho^2)(1+\beta)+\xi(3+\rho^2)]\ln\left(1+\frac{1}{1+\xi}\right) + \frac{1+2\beta+\rho^2+\xi(3-\rho^2)}{1+\xi}\right\}. \tag{1.15}$$

Here, $\mathrm{Li}_2(x)$ is the dilogarithm defined by $\mathrm{Li}_2(x) = -\mathrm{Re}\int_0^x \frac{\ln(1-t)}{t}dt$.

The difference between $|\Delta_e^N|$ and Δ_e^S had been neglected in earlier parametrizations of the pair production cross section. This difference is the effect of the difference in the screening functions $\Phi_{1,2}$ before the additional integration. In addition, the special functions in Δ_e were approximated by an expression consisting only of elementary functions in [9]. Based on the results in [11], we have separated the coefficients of the two screening functions. Incorporating the calculations for the effect of a nuclear form factor analogous to the bremsstrahlung case and [10] and adding the contribution of atomic electrons [12], we arrive at the following expression for the pair production cross section

$$\frac{d^2\sigma}{dv\,d\rho} = \frac{2}{3\pi}Z(Z+\zeta)\frac{1-v}{v}\left[\Phi_e + \frac{m_e^2}{m_\mu^2}\Phi_\mu\right], \tag{1.16}$$

where

$$\Phi_e = C_1^e L_1^e + C_2^e L_e^2, \quad C_1^e = C_e - C_2^e, \tag{1.17}$$

$$C_2^e = [(1-\rho^2)(1+\beta)+\xi(3-\rho^2)]\ln\left(1+\frac{1}{\xi}\right) + 2\frac{1-\beta-\rho^2}{1+\xi} - (3-\rho^2), \tag{1.18}$$

$$L_1^e = \ln\frac{BZ^{-1/3}\sqrt{1+\xi}}{X_e + \frac{2m_e\sqrt{e}BZ^{-1/3}(1+\xi)}{Ev(1-\rho^2)}} - \frac{\Delta_e}{C_e} - \frac{1}{2}\ln\left[X_e + \left(\frac{m_e}{m_\mu}D_n\right)^2(1+\xi)\right] \tag{1.19}$$

$$L_2^e = \ln\frac{BZ^{-1/3}e^{-1/6}\sqrt{1+\xi}}{X_e + \frac{2m_e e^{1/3}BZ^{-1/3}(1+\xi)}{Ev(1-\rho^2)}} - \frac{\Delta_e}{C_e} - \frac{1}{2}\ln\left[X_e + \left(\frac{m_e}{m_\mu}D_n\right)^2 e^{1/3}(1+\xi)\right], \quad X_e = \exp\left(-\frac{\Delta_e}{C_e}\right), \tag{1.20}$$

$$\Delta_e = [(2+\rho^2)(1+\beta)+\xi(3+\rho^2)]\,\mathrm{Li}_2\frac{1}{1+\xi} - (2+\rho^2)\xi\ln\left(1+\frac{1}{\xi}\right) - \frac{\xi+\rho^2+\beta}{1+\xi}, \tag{1.21}$$

and

$$\Phi_\mu = C_1^\mu L_1^\mu + C_2^\mu L_2^\mu, \quad C_1^\mu = C_\mu - C_2^\mu, \tag{1.22}$$

$$C_2^\mu = [(1-\beta)(1-\rho^2) - \xi(1+\rho^2)]\frac{\ln(1+\xi)}{\xi} - 2\frac{1-\beta-\rho^2}{1+\xi} + 1 - \beta - (1+\beta)\rho^2, \tag{1.23}$$

$$L_1^\mu = \ln\frac{B\frac{\mu}{m_e}Z^{-1/3}/D_n}{X_\mu + \frac{2m_e\sqrt{e}BZ^{-1/3}(1+\xi)}{Ev(1-\rho^2)}} - \frac{\Delta_\mu}{C_\mu}, \tag{1.24}$$

$$L_2^\mu = \ln\frac{B\frac{\mu}{m_e}Z^{-1/3}/D_n}{X_\mu + \frac{2m_e e^{1/3}BZ^{-1/3}(1+\xi)}{Ev(1-\rho^2)}} - \frac{\Delta_\mu}{C_\mu}, \quad X_\mu = \exp\left(-\frac{\Delta_\mu}{C_\mu}\right), \tag{1.25}$$

PoS(ICRC2019)429

Table 1: Parameters of the parametrization for the radiative corrections to the bremsstrahlung cross section.

n	0	1	2	3	4	5
a_n	-0.00349	148.84	-987.531			
b_n	0.1642	132.573	-585.361	1407.77		
c_n	-2.8922	-19.0156	57.698	-63.418	14.1166	1.84206
d_n	2134.19	581.823	-2708.85	4767.05	1.52918	0.361933

$$\begin{aligned}\Delta_\mu = &\left[(1+\rho^2)\left(1+\frac{3}{2}\beta\right) - \frac{1}{\xi}(1+2\beta)(1-\rho^2)\right]\mathrm{Li}_2\left(\frac{\xi}{1+\xi}\right) \\ &+\left(1+\frac{3}{2}\beta\right)\frac{1-\rho^2}{\xi}\ln(1+\xi) + \left[1-\rho^2-\frac{\beta}{2}(1+\rho^2)+\frac{1-\rho^2}{2\xi}\beta\right]\frac{\xi}{1+\xi}\end{aligned} \tag{1.26}$$

with the abbreviations

$$\zeta = \frac{0.073\ln\frac{E/\mu}{1+\gamma_1 Z^{2/3}E/\mu} - 0.26}{0.058\ln\frac{E/\mu}{1+\gamma_2 Z^{1/3}E/\mu} - 0.14}, \tag{1.27}$$

$$\gamma_1 = 1.95\times10^{-5}, \quad \gamma_2 = 5.3\times10^{-5} \text{ for } Z\neq 1, \tag{1.28}$$

$$\gamma_1 = 4.4\times10^{-5}, \quad \gamma_2 = 4.8\times10^{-5} \text{ for } Z = 1. \tag{1.29}$$

1.3 Radiative corrections to bremsstrahlung

The radiative corrections to the bremsstrahlung cross section have been calculated based on the Weizsäcker-Williams method and the radiative corrections to the Compton cross section [13] and the double Compton cross section [14]. In [15], some of us have calculated radiative corrections to the average energy loss. Based on this calculation we have determined the corrections to the differential cross section. The cross section factorizes into the screening function and a universal function $s_{\mathrm{rad}}(v)$ of the fractional energy loss v. The calculation on the basis of the Weizsäcker-Williams method cannot distinguish between the terms proportional to Φ_1 and Φ_2. Since this would be a small correction of a few percent to the already small radiative corrections, this does not pose a problem. Numerical calculations can be parametrized by

$$\begin{aligned}\left.\frac{d\sigma}{dv}\right|_{\mathrm{rad}} &= Z^2\alpha^2\left(r_e\frac{m_e}{\mu}\right)^2\Phi_1(\delta)s_{\mathrm{rad}}(v), \\ s_{\mathrm{rad}}(v) &= \begin{cases}\sum_{n=0}^{2} a_n v^n & v<0.02, \\ \sum_{n=0}^{3} b_n v^n & 0.02\le v<0.1, \\ \sum_{n=0}^{2} c_n v^n + c_3 v\ln v + c_4\ln(1-v) + c_5\ln^2(1-v) & 0.1\le v<0.9, \\ \sum_{n=0}^{2} d_n v^n + d_3 v\ln v + d_4\ln(1-v) + d_5\ln^2(1-v) & v\ge 0.9,\end{cases}\end{aligned} \tag{1.30}$$

where the values of the fit parameters a_n, b_n, c_n, d_n are given in Table 1.

PoS(ICRC2019)429

2. Effect of improved cross sections on muon simulations

The average energy loss of the new bremsstrahlung and pair production cross sections compared to the baseline cross sections is shown in Figure 1. An increase of around 2 % for the

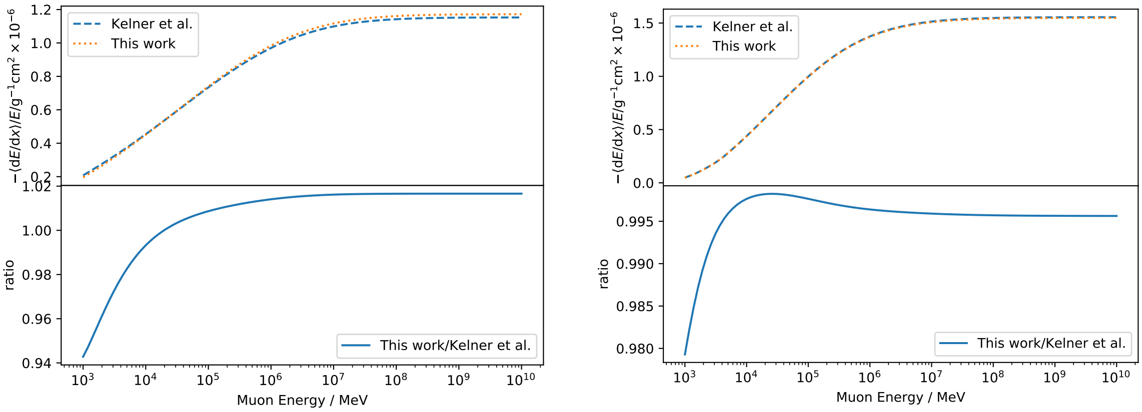

(a) Average energy loss of bremsstrahlung.

(b) Average energy loss of pair production.

Figure 1: The average energy loss of the cross sections shown above compared to Kelner et al. [7, 8, 9, 10, 12] for bremsstrahlung 1a and pair production 1b.

bremsstrahlung cross sections, mainly driven by the radiative corrections, and a slight decrease of the pair production cross section are observed. Further effects on the propagation are studied using the lepton propagator PROPOSAL.

2.1 The lepton propagator PROPOSAL

PROPOSAL [16] is a Monte-Carlo Simulation library to propagate charged leptons. It is mainly designed to simulate muons with energies above 10 GeV traveling large distances through media with high performance and accuracy. This is needed for large volume detectors like neutrino telescopes or other underground experiments dealing with an atmospheric muon background. PROPOSAL is used in the IceCube simulation chain for the propagation and decay of muons and taus.

PROPOSAL is a C++ library, originally written in Java (called MMC) [17], but through a pybinding wrapper, it can also be used as a Python library. The current version [18][1] includes a complete reconstruction to a modular code structure and polymorphism resulting in a performance improvement of 30 %. To reach a high precision in a decent amount of time, PROPOSAL uses interpolation tables during initialization. Although there is the possibility not to use the interpolations and always integrate over the propagation integrals, this decreases the performance by orders of magnitudes.

One of the main goals of PROPOSAL is the ability to do systematic studies concerning the uncertainties in the muon cross sections. Therefore multiple cross section parametrizations are available to study their effect on the propagation. Currently, there are two pair production parametrizations, five bremsstrahlung parametrizations and eight nuclear inelastic interaction parametrizations

[1]The code is available at `https://github.com/tudo-astroparticlephysics/PROPOSAL`.

PoS(ICRC2019)429

available. The production of a muon pair [19] and the weak interaction [20] are optional processes. Although the muon production doesn't contribute to the average energy loss, the additional muon tracks create a different event signature in a detector and also increase the muon flux for air showers measured on earth. The weak exchange of a charged current is even less common, but the disappearing high energy muon track in a hadronic shower and an invisible outgoing neutrino creates a unique signature inside the detector.

2.2 Effects on the range- and energy loss distribution

The effects of using different cross sections can be best seen in the distribution of the secondary particles, or the energy losses and decay products. In addition to that, the range distribution should also be affected, while being influenced more indirectly. A comparison of the bremsstrahlung and pair production cross sections calculated in this work with the widely used cross sections calculated by Kelner et al. [7, 8, 9, 10, 12] on the range and secondaries distribution using PROPOSAL is shown in figure 2.

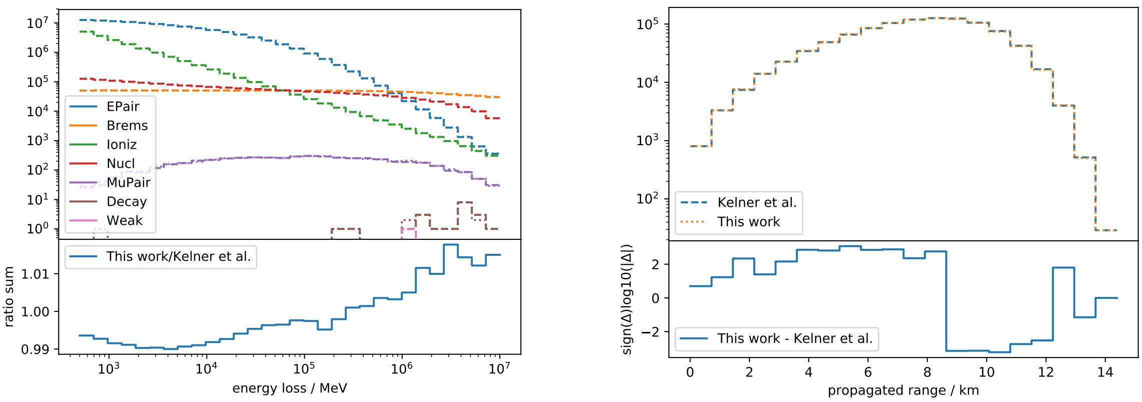

(a) Secondaries distribution of 10^7 muons propagated 100 m.

(b) Range distribution of 10^6 muons propagated until they decay.

Figure 2: Effects of the cross sections shown above (dotted) compared to Kelner et al. [7, 8, 9, 10, 12] (dashed) regarding the secondaries 2a and range 2b distribution when propagating muons with an energy of 10 TeV through ice using a minimum energy loss cut of 500 MeV.

In the secondaries distribution 2a, an increase at the higher energy losses is observed, which is expected as the new bremsstrahlung cross section is slightly higher. In addition to that, the pair production cross section is slightly lower, which increases the effect, since the bremsstrahlung dominates the higher energy losses while the pair production dominates the lower energy losses at this energy. The additional processes of muon pair production and weak interaction are negligible as well as the electrons from decays.

In the range distribution 2b, the higher range bins are decreased, which is explained by the higher cross sections. These shorter propagating muons are then distributed in the lower ranges bins, which then increases.

PoS(ICRC2019)429

3. Conclusion

New muon cross sections for bremsstrahlung and pair production with an improved description of the screening of an atom is presented showing a decrease of half a percent of the cross section. In addition radiative corrections for bremsstrahlung showing an increase of 2 % are presented. These new cross sections slightly shift the energy loss distribution to more high energy losses and less smaller losses. Also, the range distribution of the muons tends to shorter ranges.

Acknowledgments

We acknowledge funding by the Deutsche Forschungsgemeinschaft (DFG) – Project number 349068090.

References

[1] H. Bethe and W. Heitler, *Proc. Roy. Soc. Lond. A.* **146** (1934) 83.

[2] S. R. Kelner, R. P. Kokoulin, and A. A. Petrukhin, *Phys. At. Nucl.* **62** (1999) 1894–1898.

[3] A. A. Petrukhin and V. V. Shestakov, *Canad. J. Phys.* **46** (1968) S377.

[4] L. R. B. Elton, *Nuclear Sizes*. Oxford University Press, 1961.

[5] E. V. Bugaev, *Sov. Phys. J. Exp. Theor. Phys.* **45** (1977) 12–16.

[6] Y. M. Andreev and E. V. Bugaev, *Phys. Rev. D* **55** (1997) 1233–1243.

[7] S. R. Kelner, R. P. Kokoulin, and A. A. Petrukhin. Preprint MEPhI 024-95, Moscow, 1995.

[8] S. R. Kelner, R. P. Kokoulin, and A. A. Petrukhin, *Phys. At. Nucl.* **60** (1997) 576–583.

[9] R. P. Kokoulin and A. A. Petrukhin in *Proc. 11th ICCR*, vol. 29, pp. 277–284. 1969.

[10] R. P. Kokoulin and A. A. Petrukhin in *Proc. 12th ICCR*, vol. 6, pp. 2436–2444. 1971.

[11] S. R. Kelner, *Sov. J. Nucl. Phys.* **5** (1967) 778.

[12] S. R. Kelner, *Phys. At. Nucl.* **61** (1998) 448–456.

[13] L. M. Brown and R. P. Feynman, *Phys. Rev.* **85** (1952) 231.

[14] F. Mandl and T. H. R. Skyrme, *Proc. Roy. Soc. Lond. A Math. Phys. Sci.* **215** (1952) 497.

[15] A. Sandrock, S. R. Kelner, and W. Rhode, *Phys. Lett. B* **776** (2018) 350–354.

[16] J.-H. Koehne et al., *Comput. Phys. Commun.* **184** (2013) 2070–2090.

[17] D. Chirkin and W. Rhode. arXiv:hep-ph/0407075, 2004.

[18] M. Dunsch et al., *Comput. Phys. Commun.* **242** (2019) 132–144.

[19] S. R. Kelner, R. P. Kokoulin, and A. A. Petruhkin, *Phys. At. Nucl.* **63** (2000) 1603–1611.

[20] A. Sandrock. PhD thesis, TU Dortmund, 2018.

PoS(ICRC2019)429